 FDMP, vol.6, no.2, pp.219-232, 2010

The Influence of Annealing in Nitrogen Atmosphere on the Electrical, Optical and Structural Properties of Spray-Deposited ZnO Thin Films

Shadia J Ikhmayies[1], Naseem M. Abu El-Haija[2] and Riyad N. Ahmad-Bitar[3]

Abstract: Large area and highly uniform polycrystalline ZnO thin films have been produced by a spray pyrolysis (SP) technique resorting to a customized system (spraying) on glass substrates at temperature T_s = 450°C. This study deals with the related investigation about the influence of heat treatment (in nitrogen atmosphere) on the resulting properties (electrical, optical and structural) of such films. Properties are analyzed by means of I-V plots, transmittance curves, X-Ray diffractograms (XRD) and scanning electron microscope (SEM) micrographs. Results show that the resistivity of the films decreases from about 200 Ω.cm for the as-deposited films to about 95 Ω.cm for annealed films. XRD diffractograms reveal that the films are polycrystalline with a hexagonal wurtzite structure. The preferential orientation (002) does not change with annealing, but some very weak lines appear, as witnessed by the XRD patterns. According to such patterns and SEM images there is no noticeable increase in the grain size. The transmittance of the films increases as a result of annealing beside a slight increase in the bandgap energy. From the analysis of the Urbach tail at the absorption edge, the width of the tail of localized states E_e is 1.084 eV for the as-deposited film and 1.126 eV for the annealed film. The large values of E_e depend on localized states resulting from oxygen defects that increase with annealing.

Keywords: Spray pyrolysis, annealing, ZnO thin films, solar cells, Urbach tail.

1 Introduction

Zinc oxide is a semiconducting material with a crystalline structure of the wurtzite type, having constants of the crystalline unit cell a = 3.24Å and c = 5.19Å, respectively [Rusu and Rusu (1999-2000)]. Undoped ZnO films are known to exhibit

[1] Physics Department, Faculty of Science, University of Jordan, Amman-Jordan. E-mail: shadia_ikhmayies@yahoo.com

[2] Physics Department, Faculty of Science, University of Jordan, Amman-Jordan.

[3] Physics Department, Faculty of Science, University of Jordan, Amman-Jordan.

n-type conductivity that is usually ascribed to oxygen vacancies in the crystallites [Studenikin.; Golego and Cocivera (1998 a)]. Thin-film zinc oxide continues to attract attention because of its low toxicity and its many applications in solar cell technology. That is, it is a serious candidate for the substitution of indium tin oxide and tin oxide in the manufacture of conductive electrodes of the solar cells due to its high stability. Also it has many applications as thin-film gas sensors, varistors, and a phosphor for color displays [Studenikin.; Golego and Cocivera (1998 a)].

There are various methods for the preparation of ZnO thin films such as thermal evaporation [Fouad; Ismail; Zaki and Mohamed (2006)], rf-sputtering [Song (2008)], atomic layer deposition [Saito; Watanabe; Takahashi; Matsuzawa; Sang and Konagai (1997)], chemical vapor deposition [Natsume; Sakata and Hirayama (1995)], sol-gel [Musat; Rego; Monteiro and Fortunato (2008)], laser ablation [Singh; Mehra; Yoshida and Wakahara (2004)] and spray pyrolysis (SP) technique [Studenikin; Golego and Cocivera (1998 a); Studenikin; Golego and Cocivera (1998 b); Ikhmayies (2002); Studenikin; Golego and Cocivera (2000)]. The last one has received attention because of its simplicity and consequent economics as it does not require a high vacuum apparatus. Also, it enables the production of large area and highly transparent films beside the ability to make intentional doping simply by adding the dopant compound to the precursor solution.

The electrical properties of ZnO can be modified by thermal treatment with different atmospheres; such as hydrogen and nitrogen. Many workers made annealing of ZnO thin films, for example; Studenikin; Golego and Cocivera (1998 a) made annealing in nitrogen, Studenikin; Golego and Cocivera (1998 b) made annealing in a forming gas ambient (N_2: H_2 = 95: 5), Studenikin; Golego and Cocivera (2000) made annealing in hydrogen and oxygen and Rusu and Rusu (1999-2000) made annealing in vacuum and oxygen atmosphere. But annealing in oxygen atmosphere was found by those authors [Rusu and Rusu (1999-2000); Studenikin; Golego and Cocivera (2000)] to reduce the electrical conductivity. In this work, ZnO thin films were annealed in nitrogen atmosphere and an improvement in the electrical, optical and structural properties was obtained. So, it was shown that this treatment improves the quality of the ZnO thin films.

2 Experimental

Some authors used zinc nitrate to prepare ZnO thin films, such as Studenikin; Golego and Cocivera (1998 a) and Studenikin; Golego and Cocivera (1998 b). Other authors used zinc acetate, such as Sanchez-Juarez; Tiburcio-Silver and Ortiz (1998) and Lokhande and Uplane (2000), and others used zinc chloride such as Ebothé; El Hichou; Vautrot and Addou (2003) and Ikhmayies; Abu El-Haija and Ahmad-Bitar (2010). In this work zinc chloride (0.8% - 2.5% varying con-

centration) was used to prepare the precursor solution for ZnO thin films, where 7.37×10^{-3} mole of $ZnCl_2$ was dissolved in 600 ml of distilled water.

The home-made spray pyrolysis apparatus used in this work was described in elsewhere [Ikhmayies (2002)]. The spraying process was done intermittently (each 5 minutes the spraying continues for 10s) and the total spraying time was 5-8 hours. We found that this is the best way to produce highly transparent and polycrystalline ZnO thin films.

The substrates are micro slides of ordinary glass of dimensions $2.5\times6\times0.1$ cm^3. These slides were cleaned by dipping in distilled water then by an ultrasonic cleaner while soaked in methanol for (20 – 30) min, and again soaked in distilled water and finally polished with lens papers.

The solution spray rate was in the range (3-5) ml/min. The optimum carrier gas pressure for this rate of solution flow was around $5kg/cm^3$. Nitrogen N_2 was used as the propelling gas. The nozzle substrate distance was adjusted to get the largest uniform area which was about 30 cm in diameter. The substrate temperature was 450˚C, and the films were annealed in nitrogen atmosphere at 250°C by using an annealing system that was described in elsewhere [Ikhmayies (2002)].

The I-V measurements were taken in the dark at room temperature by a system that consists of a Keithley 2400 Source Meter capable of measuring 10^{-11}A, which was interfaced by an IBM computer. The sample in question was placed in a brass cell which enables us of taking the measurements in the dark. Aluminum was used as the contact material for ZnO thin films. Two strips of aluminum were deposited on the surface of the film by vacuum evaporation. The strips had a length of 1 cm, width of 2 mm, and separation of 3 mm.

The transmittance of the films was measured in the wavelength range $\lambda = 290 - 1100nm$ by using a double beam Shimadzu UV 1601 (PC) spectrophotometer with respect to a piece of glass of the same kind of the substrates. The minima and maxima in the transmittance curves were used to estimate the film thickness as follows, [Goodman (1978)]:

Consider the transmittance at a certain maximum as $T_{\max}$, the transmittance at the next minimum as $T_{\min}$ and dispersion is negligible, then define a parameter ρ_T by the approximate form,

$$\rho_T = \frac{T_{\max}}{T_{\min}} \cong \left[\frac{\left(n_1^2 + n_0^2\right)\left(n_1^2 + n_2^2\right)}{2n_1^2\left(n_0^2 + n_2^2\right)} \right] \tag{1}$$

where n_0, n_1, and n_2 are the refractive indices of air, film, and glass respectively,

and the condition $n_0 \prec n_1$ and $n_2 < n_1$ was satisfied. Solving (1) for n_1 to have

$$n_1 = \left\{ \frac{-\left(n_0^2+n_2^2\right)(1-2\rho_T) + \left[\left(n_0^2+n_2^2\right)(1-2\rho_T)^2 - 4n_0^2n_2^2\right]^{\frac{1}{2}}}{2} \right\}^{\frac{1}{2}} \tag{2}$$

and the film thickness is given by

$$t = \frac{\lambda_{\max} \cdot \lambda_{\min}}{4n_1\left(\lambda_{\min} - \lambda_{\max}\right)} \tag{3}$$

where $\lambda_{\min}$ and $\lambda_{\max}$ are the values of the wavelength at a certain maximum and the next minimum respectively. The estimated value of film thickness is about 400 nm.

X-ray measurements were made with a Philips PW1840 Compact X-ray diffractometer system with Cu K_α (λ = 1.5405 Å). The measurements were recorded at a diffraction angle 2θ from 30° to 82°. The SEM images were taken by a LEITZ-AMR 1000A scanning electron microscope.

3 Results and Discussion

3.1 Electrical Properties

It is well known that ZnO films made without any intentional doping exhibit n-type conductivity, caused by a deviation from stoichiometry due to native defects. Traditionally, two intrinsic defects most commonly are reported in the literature as dominant background donors in ZnO, namely the oxygen vacancy (V_O) and interstitial Zn (Zn_I) [Song (2008)].

Undoped ZnO thin films prepared in this work on glass substrates by the spray pyrolysis (SP) technique have been submitted to a thermal treatment in nitrogen atmosphere at 250°C for 45 minutes. Fig.1 shows the I-V characteristics for one undoped ZnO thin film deposited at T_s = 450°C before and after annealing. The resistivity was estimated by using the slopes of the I-V curves which are linear. It had decreased from about 200 Ω.cm for the as-deposited film to about 95 Ω.cm for the annealed film or a decrease by a factor of 2.1. The reduction of the resistivity after annealing is due to the removal of oxygen from the films and hence the creation of oxygen vacancies. In other words, annealing tends to produce oxygen defects, which are donors of electrons.

These high values of the resistivity may be attributed to the high substrate temperature which is 450°C, which results in an approximately perfect ZnO films

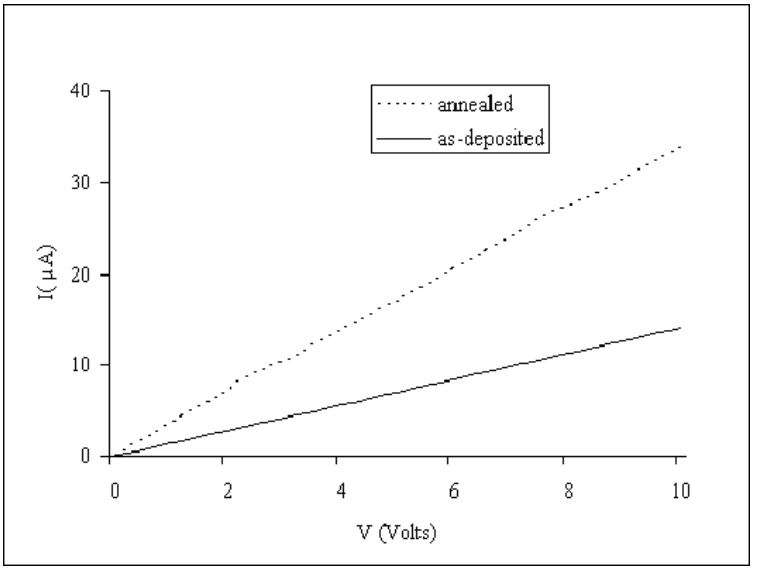

Figure 1: I-V plots for a thin film of ZnO before and after annealing in nitrogen atmosphere at T = 250°C for 45 min.

(i.e. free from defects which reduce the resistivity). Some authors got larger values of the resistivity, for example Studenikin; Golego and Cocivera (1998 a) got 10^4 Ω.cm for spray-deposited ZnO thin films after annealing in nitrogen ambient. Musat; Rego; Monteiro and Fortunato (2008) got electrical resistivity between $6 \times 10^6 - 7 \times 10^7 \Omega$.cm for ZnO thin films prepared by sol-gel and annealed in N_2. Other authors got smaller values of the resistivity such as Mazón; Muci; Sa-Neto; Ortiz-Conde and Jarcía (1991) who got values of the resistivity in the range $3.2 \times 10^{-3} - 1.5 \times 10^{-2} \Omega.cm$ for ZnO films prepared by the SP technique. Yang; Sun W. X.; Chen J. B.; Xu; Chen P. T.; Sun Q. C.; Tay and Sun Z. (2006) got $2.44 \times 10^{-3} \Omega$.cm by using vacuum arc deposition technique and Saito; Watanabe; Takahashi; Matsuzawa; Sang and Konagai (1997) got 6.9×10^{-4} Ω.cm by the photo atomic layer deposition (photo-ALD) method without any intentional doping.

3.2 Optical Properties

Fig.2 depicts the transmittance curves for a film of thickness about 400 nm before and after annealing. As the figure shows, the transmittance is larger than 80% before and after heat treatment. Since the electrical resistivity was decreased, the optical properties are expected to be improved after annealing. The transmittance had increased after annealing in the whole wavelength range, i.e. in the visible and

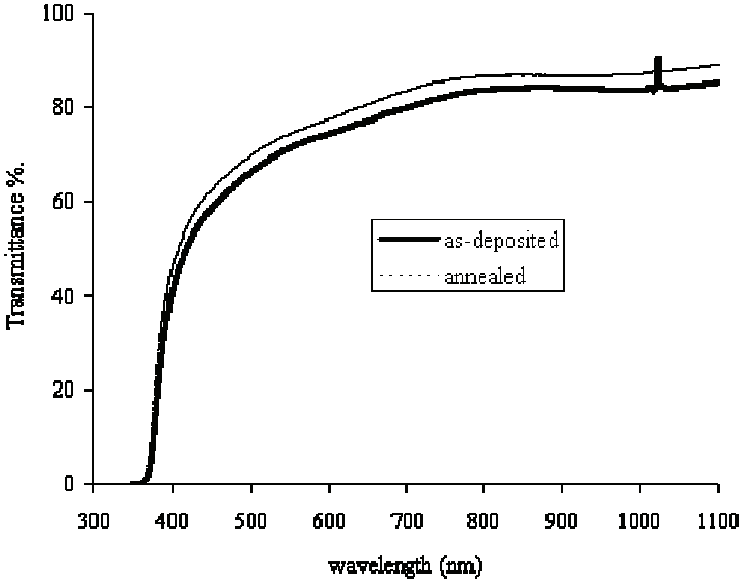

Figure 2: Transmittance of ZnO thin films before and after annealing in nitrogen atmosphere at 250°C for 45 minutes.

infrared domains. This rise in transmittance may be due to the removal of a surface layer or the improvement of the surface by annealing. From the transmittance of the as-deposited and annealed films around the band edge in the lower energy side, large tailing could be observed. This tailing could be attributed to the zinc interstitial and oxygen interstitial energy levels near the band edge.

Fig.3 depicts the relation between the absorption coefficient α and the radiation energy hν, where h is Planck's constant and ν is the frequency of the radiation. It is noticed that the absorption coefficient was rapidly increasing after the absorption edge, and that annealing had decreased it in the whole energy range. In the low energy range tailing near the absorption edge is noticeable for the as-deposited film and the film after annealing. The presence of spikes in the absorption coefficient at high energies (close to 3.5 eV) could be related to the formation of quantum dots. Also the decrease in the absorption coefficient in this region which is more apparent after annealing is due to the formation of nanocrystallites. The formation of nanocrystallites results in larger optical bandgap energy and then smaller absorption of light.

A plot of $(\alpha h\nu)^2$ versus (hν) (Fig.4) was used to estimate the bandgap energy E_g. Before annealing the bandgap energy was E_g =3.27 eV but after annealing it became E_g = 3.28 eV. So there is a slight increase in the bandgap energy after

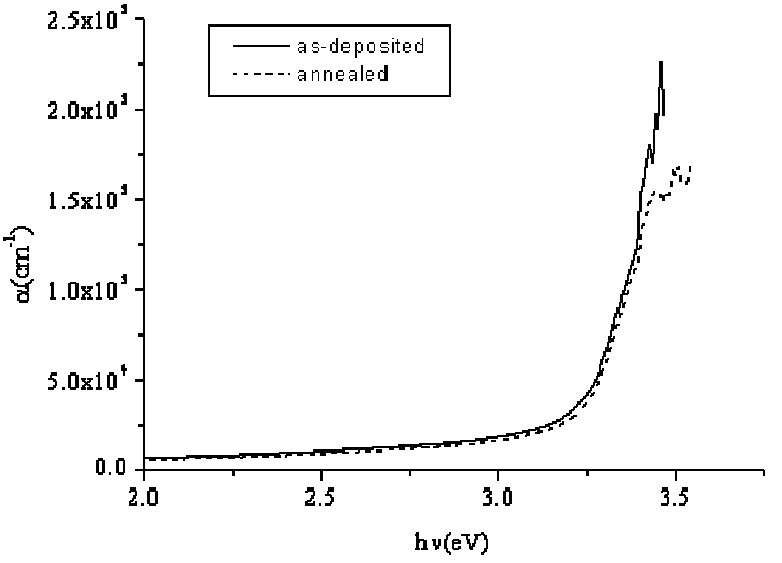

Figure 3: The relation between the absorption coefficient α and the radiation energy hν for ZnO thin films.

annealing, which may mean a slight decrease in the lattice spacing d, that is the size of the crystal lattice decreases after the removal of oxygen, and it is well known that the lattice spacing d and bandgap go in opposite directions. But at the same time annealing helps to move the interstitial Zn to fill the Zn vacancy in the lattice, and the effect of this is to increase d, so we have two opposite effects one decreases d (removal of oxygen) and another increases it (the filling of Zn vacancy due to the motion of Zn interstitial) which results in a slight change in the bandgap energy. These results are consistent with the results of Studenikin; Golego and Cocivera (1998 a) where they concluded that annealing brought all the samples to the same band gap 3.30 eV.

The absorption coefficient α in the low energy range empirically follows the exponential law, i.e. the Urbach tail expressed by [Natsume; Sakata and Hirayama (1995)]

$$\alpha(\omega) = \alpha_0 \exp(\hbar\omega/E_e) \tag{4}$$

Where α_0 is a constant, ω the angular frequency of the radiation, and E_e an energy which is a constant or according to Natsume; Sakata and Hirayama (1995) weakly dependent on temperature and often interpreted as the width of the tail of localized states in the bandgap. The relation between ln(α) against the radiation energy hν

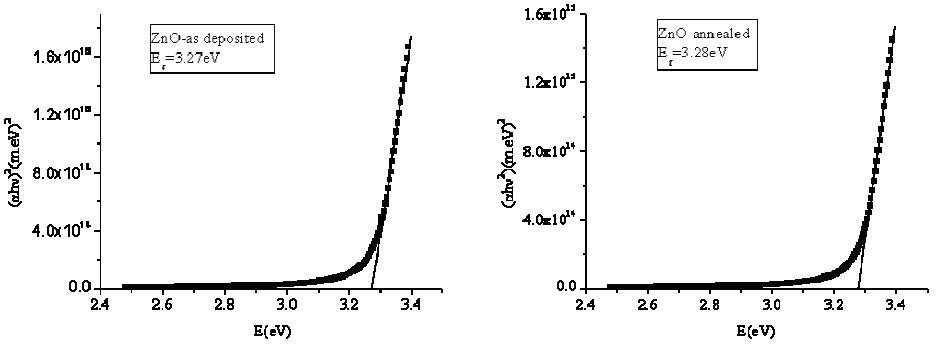

(a) (b)

Figure 4: The plot of $(\alpha h\nu)^2$ versus the photon's energy $h\nu$ for ZnO thin films. a) As deposited. b) Annealed.

is shown in Fig. 5. As the figure shows a linear region is observed between 1.47 eV and 2.92 eV which can be fitted by a straight line. The width of the Urbach tail equals the inverse of the slope of the obtained straight line in each case. The obtained values are 1.084 eV for the as-deposited film and 1.126 eV for the annealed film. So, the films had shown large band tails, which are most probably attributed to the disorder caused by the existence of interstitial Zinc atoms and may be interstitial oxygen atoms too. As a result, localization of electrons due to the disorder was expected. These values are much larger than the values obtained by Natsume; Sakata and Hirayama (1995) for ZnO films prepared by chemical vapor deposition, where there values are in the range 0.08-0.10 eV. The width of Urbach tail had increased after annealing, which could be related to the increase of oxygen defects after annealing and these may include oxygen interstitials which cause large band tails [Xu; Lau; Chen and Tay (2001)].

3.3 Structural Properties

3.3.1 X-Ray Diffractograms

X-ray diffraction patterns of undoped ZnO thin films before and after annealing in nitrogen atmosphere at 250˚C are shown in Fig.6. As the figure shows the ZnO films are polycrystalline, and the diffraction peaks can be indexed to hexagonal wurtzite structured ZnO. The intensity of the peaks relative to the background signal demonstrates the high crystallinity of the ZnO films produced by the SP technique.

The orientation of crystal growth is mainly in the (002) plane which indicates that

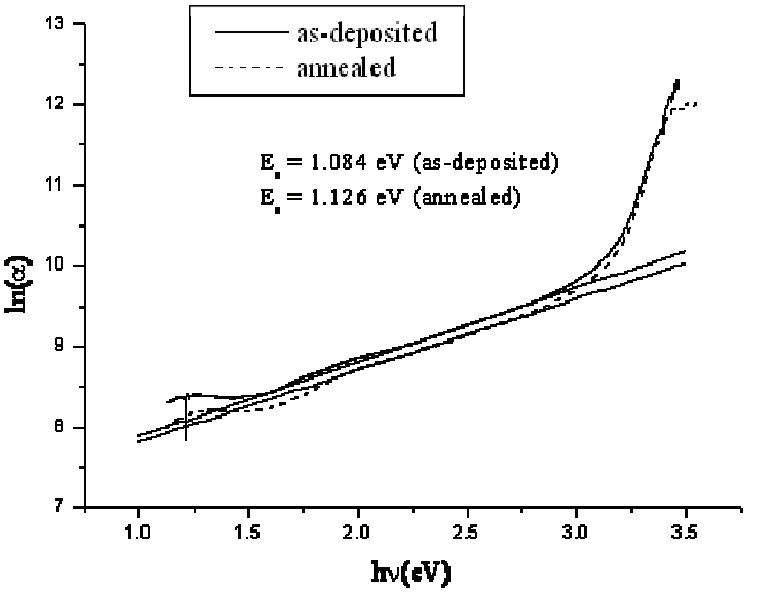

Figure 5: The plot and linear fit of ln(α) versus hν for ZnO thin films.

the c-axes of the grains are perpendicular to the substrate surface. Other peaks with much smaller intensity are also observed which correspond to the reflections from the (100), (101), (102), (103) and (004) planes. Our results are in good agreement with the results of Studenikin; Golego and Cocivera (1998 a) for ZnO films prepared by the spray pyrolysis technique at substrate temperatures 250 and 360°C where they used zinc nitrate in the precursor solution. These authors found that films grown by the SP technique at higher than 200˚C exhibit predominantly one peak which is the (002) showing a very high level of orientation along the *c*-axis perpendicular to the substrate. Our results are consistent with the results of Sanchez-Juarez; Tiburcio-Silver and Ortiz (1998) for their spray-deposited films prepared by using zinc acetate, who say that the (002) preferred orientation has been observed for $T_s \geq 400^{circ}$C for ZnO films prepared by the spray pyrolysis technique and that other peaks (102) and (103) are also observed, but their intensity is very small compared to that of the (002) peak. Also these results are consistent with the results obtained by Ebothé; El Hichou; Vautrot and Addou (2003), where they got a single orientation which is the (002) line and their films are spray-deposited by using zinc chloride. But this is different from the result obtained by Lokhande and Uplane (2000) who got polycrystalline spray-deposited ZnO films having hexagonal wurtzite type lattice, but with the (100) as the unique and preferred orientation,

where their films were deposited by using zinc acetate and deposited at 698K. From this we conclude that zinc compounds used in the precursor solution of the films have no effect on the preferential orientations in the XRD diffractograms. Annealing did not change the preferential orientation or the directions of crystal growth, but slightly increases the intensities of the other lines especially the (103) line.

The grain size was calculated by using Scherrer formula and the line (002) in the XRD patterns.

$$d = \frac{\lambda}{D\cos\theta} \tag{5}$$

where d is the grain size, λ is the X-ray wavelength used, D is the angular line width of the half-maximum intensity and θ is the Bragg angle. The result is that the grain size is about 30 nm before and after annealing which is in the same range given by Studenikin; Golego and Cocivera (1998 a). Studenikin; Golego and Cocivera (1998 a) found that the crystallite mean diameter- as determined from X-ray diffraction linewidth- had increased exponentially with the annealing temperature, but in our work there is no significant change in the crystallite size with annealing. The reason is that our films are deposited at high substrate temperature T_s = 450°C, but their films were prepared at low substrate temperature (around 200°C). This means that there is no noticeable effect of annealing on the grain size when the films are prepared at high substrate temperatures.

It should be noticed that the weak lines in the XRD diffractograms refer to the presence of crystallites of much smaller size than 30 nm, which is the averge grain size estimated from the (002) line. So the spray-deposited ZnO thin films contain nanocrystallites, which is consistent with our former expectation from the curve of the absorption coefficient α against the photon's energy.

3.3.2 SEM Images

The surface morphology of the films was determined by means of a scanning electron microscope. Fig.7 displays the image for one ZnO thin film before and after annealing in nitrogen at 250°C for 45 min. A complete coverage of the substrate surface by the grains was observed in both images beside the uniform surfaces in the two cases. From the comparison between the two images taking into account the difference in magnification, it could be noticed that the density of large grains had increased after annealing, which is due to the enlargement of small grains, a result that could be concluded from the growth of the weak lines in the XRD diffractograms after annealing. The size of the grains in the SEM images appears to be larger than that estimated from the XRD diffractograms and Sherrer's formula, which means that each of these grains is an aggregate of small crystals.

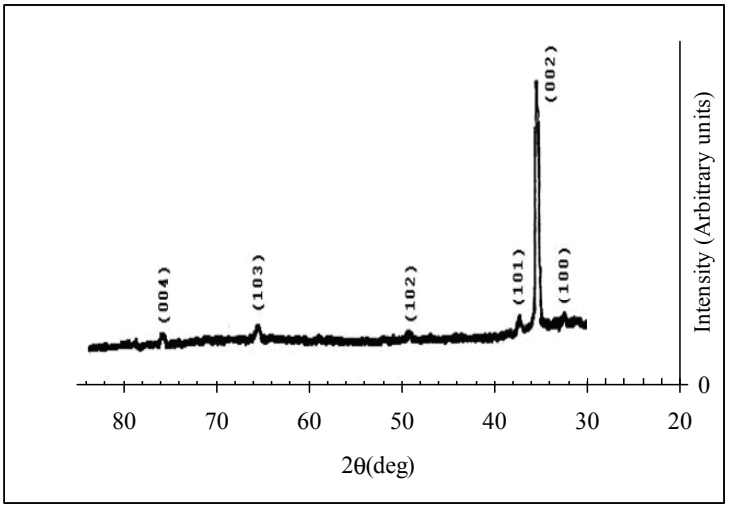

(a)

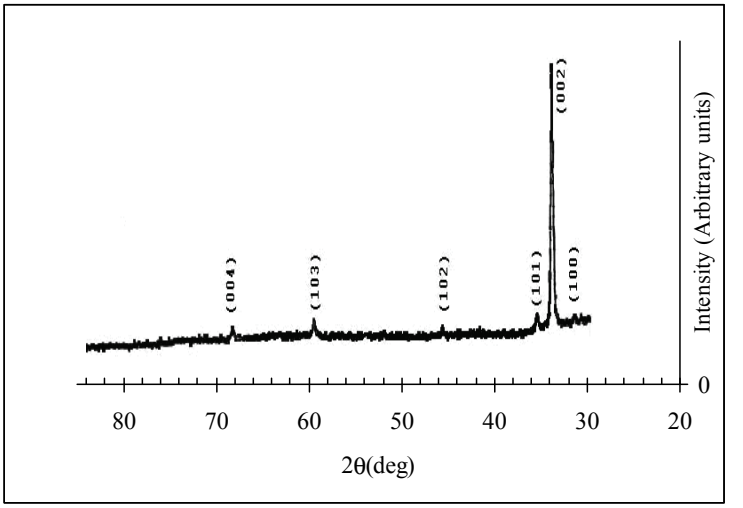

(b)

Figure 6: X-Ray diffraction patterns for ZnO thin films. a) As deposited. b) Annealed at 250°C for 45 min.

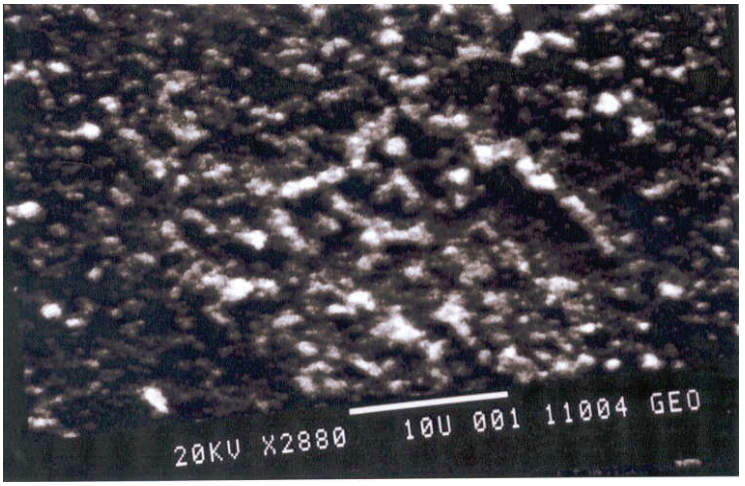

(a)

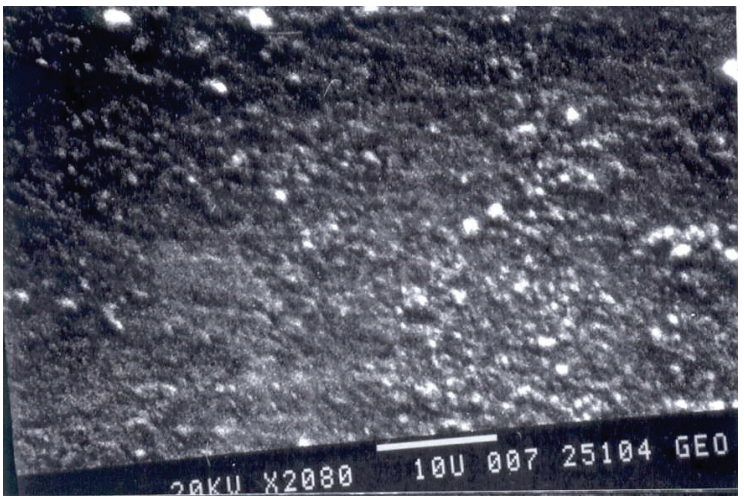

(b)

Figure 7: SEM images of un-doped ZnO thin films. a) Before annealing. (b) After annealing.

4 Conclusions

It has been shown that post-deposition annealing can play a role of crucial importance towards the end of improving the quality of films. The electrical properties of the considered films have been improved due to a decrease in the resistivity.

In particular, the structural properties have been improved as shown in the XRD

diffractograms and the SEM images due to the growth of small grains.

The Urbach tail width was estimated and was found to increase after annealing. The presence of nanocrystallites of size much smaller than 30 nm was evidenced by weak lines in the XRD diffractograms and spikes in the curve of the absorption coefficient against radiation energy.

Acknowledgement: We thank Sammeer Farrash from the physics department in the University of Jordan for depositing the electrodes by vacuum evaporation. We also thank Marsil Imsais and Khalil Tadros from the geology department in the University of Jordan too for the XRD measurements and SEM images respectively.

References

Ebothé J.; El Hichou A.; Vautrot P.; Addou M. (2003): Flow rate and interface roughness of zinc oxide thin films deposited by spray pyrolysis technique. *Journal of Applied Physics*, vol. 93, no. 1, pp. 632-640.

Fouad A. O.; Ismail A. A.; Zaki I. Z; Mohamed M. R. (2006): Zinc oxide thin films prepared by thermal evaporation deposition and its photocatalytic activity. *Applied Catalysis B: Environmental*, vol. 62, pp. 144–149.

Goodman M. Alvin (1978): Optical interference method for the approximate determination of refractive index and thickness of a transparent layer. *Applied Optics*, vol. 17, no. 17, pp. 2779-2787.

Ikhmayies J. Shadia (2002): *Production and characterization of CdS/CdTe thin film photovoltaic solar cells of potential industrial use*. Ph.D Thesis, University of Jordan, Jordan.

Ikhmayies J. Shadia; Abu El-Haija M. Naseem; Ahmad-Bitar N. Riyad (2010): Electrical and optical properties of ZnO:Al thin film prepared by the spray pyrolysis technique. *Physica Scripta*, vol. 81, doi:10.1088/0031-8949/81/01/015703.

Lokhande J. B.; Uplane D. M. (2000): Structural, optical and electrical studies on spray deposited highly oriented ZnO films. *Applied Surface Science*, vol. 167, pp. 243-246.

Mazón C.; Muci J.; Sa-Neto A.; Ortiz-Conde A.; Jarcía J. F. (1991): Spray Pyrolysis of ZnO thin films for photovoltaic applications: Effect of gas flow rate and solute concentration. *IEEE*, pp. 1156-1161.

Musat V.; Rego M. A.; Monteiro R.; Fortunato E. (2008): Microstructure and gas-sensing properties of sol-gel ZnO thin films. *Thin Solid Films*, vol. 516, pp. 1512-1515.

Natsume Y.; Sakata H.; Hirayama T. (1995): Low-Temperature electrical con-

ductivity and optical absorption edge of ZnO films prepared by chemical vapour deposition. *phys. stat. Sol. (a)*, vol. 148, pp. 485-495.

Rusu I. D.; Rusu I. I. (1999-2000): The influence of heat treatment on the electrical conductivity of ZnO thin films, *Analele Stiintifice Ale Universitatii, Fizica Strii Condensate*, pp. 113–118.

Saito Koki; Watanabe Yuki; Takahashi Kiyoshi; Matsuzawa Takeo; Sang Baosheng; Konagai Makoto (1997): Photo atomic layer deposition of transparent conductive ZnO films. *Solar Energy Materrials and Solar Cells*, vol. 49, pp. 187-193.

Sanchez-Juarez A.; Tiburcio-Silver A.; Ortiz A. (1998): Properties of fluorine-doped ZnO deposited onto glass by spray pyrolysis. *Solar Energy Materials and Solar Cells*, vol. 52, pp. 301-311.

Singh V. A.; Mehra M. R.; Yoshida A.; Wakahara A. (2004): Doping mechanism in aluminium doped zinc oxide films. *Journal of Applied Physics*, vol. 95, no. 7, pp. 3640-3643.

Song Dengyuan (2008): Effects of rf power on surface-morphological, structural and electrical properties of aluminium doped zinc oxide films by magnetron sputtering. *Applied Surface Science*, vol. 254, pp. 4171-4178.

Studenikin A. S.; Golego Nickolay; Cocivera Michael. (1998 a): Optical and electrical properties of undoped ZnO films grown by spray pyrolysis of zinc nitrate solution. *Journal of Applied Physics*, vol. 83, no. 4, pp. 2104-2111.

Studenikin A. S.; Golego Nickolay; Cocivera Michael (1998 b): Fabrication of green and orange photoluminescent, undoped ZnO films using spray pyrolysis. *Journal of Applied physics*, vol. 84, no. 4, pp. 2287-2294.

Studenikin A. S.; Golego Nickolay; Cocivera Michael (2000): Carrier mobility and density contributions to photoconductivity transients in polycrystalline ZnO films. *Journal of Applied physics*, vol. 87, no. 5, pp. 2413-2421.

Xu L. X.; Lau P. S.; Chen S. J.; Tay K. B. (2001): Polycrystalline ZnO thin films on Si (100) deposited by filtered cathodic vacuum arc. *Journal of Crystal Growth*, vol. 223, pp. 201-205.

Yang Y.; Sun W. X.; Chen J. B.; Xu X. C.; Chen P. T.; Sun Q. C.; Tay K. B.; Sun Z. (2006): Refractive indices of textured indium tin oxide and zinc oxide thin films. *Thin Solid Films*, vol. 510, pp. 95-101.